AIP Applied Physics Letters

Electrically driven integrated photonic crystal nanocavity coupled surface emitting laser

Shih-Chieh Huang, Tsung-Hua Yang, Chien-Ping Lee, and Sheng-Di Lin

Citation: Applied Physics Letters **90**, 151121 (2007); doi: 10.1063/1.2721372
View online: http://dx.doi.org/10.1063/1.2721372
View Table of Contents: http://scitation.aip.org/content/aip/journal/apl/90/15?ver=pdfcov
Published by the AIP Publishing

Electrically driven integrated photonic crystal nanocavity coupled surface emitting laser

Shih-Chieh Huang,[a] Tsung-Hua Yang, Chien-Ping Lee, and Sheng-Di Lin
Department of Electronics Engineering, National Chiao Tung University, 1001 Ta Hsueh Road, Hsin Chu 300, Taiwan

(Received 6 December 2006; accepted 8 March 2007; published online 13 April 2007)

Single mode surface emitting lasers with photonic crystal nanocavities integrated with electrically driven strained quantum well laser diodes are demonstrated. The photonic crystal serves as an end mirror for the laser cavity, while the nanocavities serve as wavelength selective high Q surface emitters. The laser emission from the nanocavities had excellent temperature stability. The wavelength shift versus temperature was about five times better than that of regular quantum well lasers. Dual wavelength emission from two side by side slightly different cavities was also demonstrated. Laser emission with two wavelengths of $\Delta\lambda = 0.8$ nm was obtained. © *2007 American Institute of Physics*. [DOI: 10.1063/1.2721372]

The concept of photonic crystal (PhC) has opened up a new way for manipulation and control of light in both passive and active photonic devices.[1,2] Coupled with the modern nanofabrication techniques, the photonic crystal devices have found applications in optical communications,[3–6] quantum information processing,[7–9] display, etc. Defects or vacancies in photonic crystal are natural high Q resonators that can trap light and serve as laser cavities.[10–12] Defect mode lasers have been demonstrated first by optical pumping[13] and then by electrical injection.[14] Nanocavities formed in photonic crystals have been proposed to be used as channel add/drop filters in wavelength division multiplexing (WDM) applications.[15–17] The resonant wavelengths of the cavities can be easily tailored to selectively pick up signals with specific wavelengths. Photonic waveguides with nanocavity add/drop couplers have been experimentally demonstrated. The work, however, was all based on light coupling from a passive waveguide and an external light source. On the other hand, stand alone nanocavity surface emitting lasers have been demonstrated.[13] But most of them were operated under optical pumping. Very few electrical pumping PhC nanocavity lasers were reported because of the difficulty in device fabrication.

In this letter, we demonstrate an integrated laser-nanocavity structure, where the laser light is directly coupled to the PhC nanocavities. Since the laser light is generated by a lateral cavity similar to a conventional edge-emitting laser, electrical pumping is easily achieved like a regular laser diode. A two-dimensional (2D) PhC slab with point defects, which were created as nanocavities, was used as a reflective mirror for the in-plane laser light, while the nanocavities served as couplers for light trapping and emission. Under the electrically driven pulse operation, the characteristics of the strongly coupled surface emitting laser light from the nanocavities were analyzed. Temperature dependence of the laser emission from the nanocavity was also measured. In addition, two side by side nanocavities with slightly different designs were fabricated to demonstrate the multiple wavelength emission capability of this integrated structure. Two surface emitting single mode lasers derived from the same in-plane laser with a wavelength separation of 0.8 nm were obtained.

Figure 1(a) shows the schematic of an integrated PhC nanocavity coupled laser structure. Strained InGaAs/GaAs single quantum well structure grown by metal organic chemical vapor deposition emitting at wavelength of 990 nm was used as the lasing media. A ridge of 1500 μm long and 20 μm wide was used as the Fabry-Pérot laser cavity. While one end of the ridge was a cleaved facet, the other end was a 2D PhC slab, which was used as the other mirror of the laser. The ridge mesa was formed by chemical etching, which

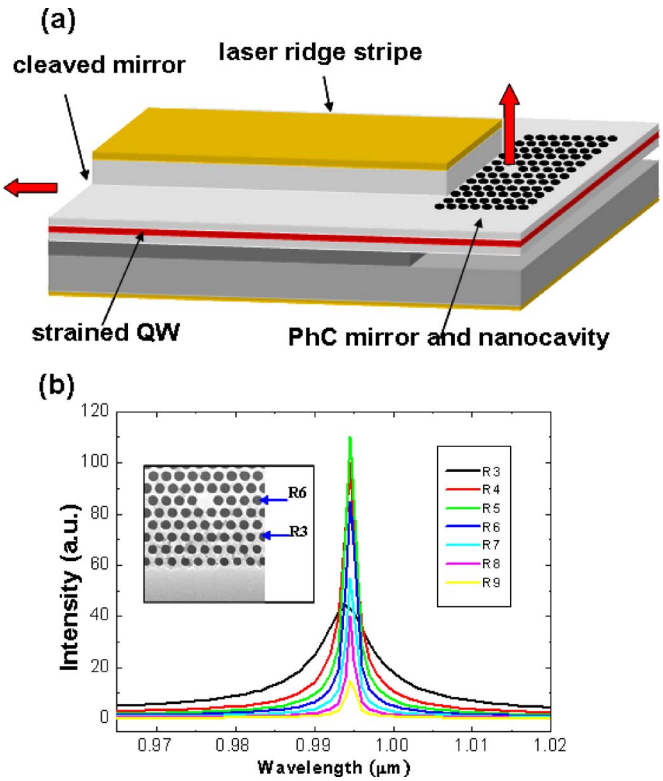

FIG. 1. (Color online) (a) Schematic of an integrated nanocavity coupled surface emitting laser. (b) Calculated position dependence of coupled output light intensity from an H1 nanocavity. The Rn ($n=1,2,\ldots,9$) represents the row from which a hole is removed. The inset shows the position of a fabricated H1 nanocavity at the sixth row.

[a]FAX: +886-3-5724361; electronic mail: schuang.ee91g@nctu.edu.tw

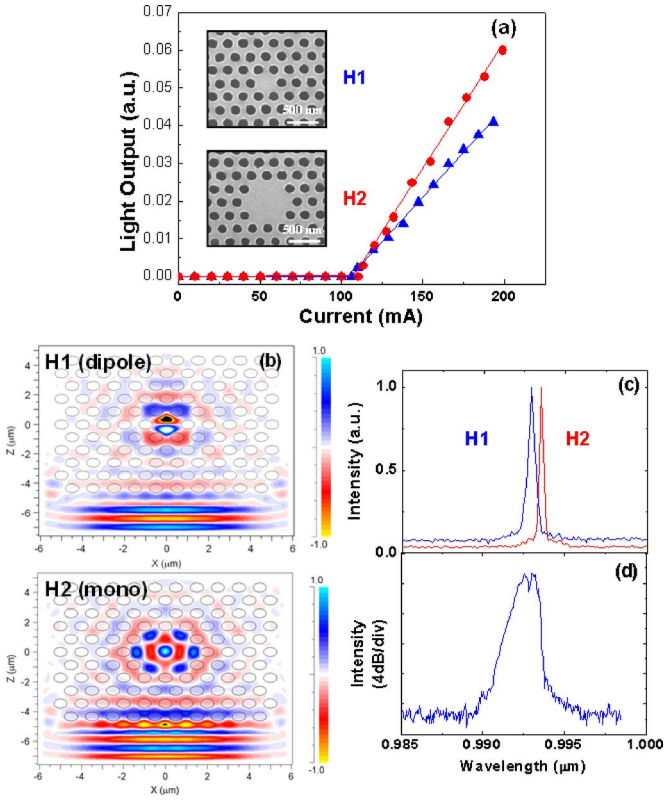

FIG. 2. (Color online) (a) *L-I* curve of laser emission from the H1 (blue triangle) and H2 (red dot) cavities. The inset shows the SEM pictures of H1 and H2 cavities. (b) Resonant cavity modes simulated by 2D FDTD method. (c) Spectra measured from the nanocavity. Blue curve: the laser with an H1 cavity. Red curve: the laser with an H2 cavity. (d) The spectrum measured from the cleaved facet of the laser diode with an H1 nanocavity. A clear dip at $\lambda=992.8$ nm exactly corresponds to the emission peak of the H1 nanocavity. The laser was driven with an injection current $I=175$ mA $(=1.6I_{th})$.

created a height of 1.1 μm and stopped in the upper cladding layer of the laser structure. Conventional processing techniques were used for the ridge waveguide fabrication. *P*-type metal of Ti/Pt/Au and *n*-type metal of Ni/Ge/Au were deposited on the top of the ridge mesa and at the bottom of the laser structure for Ohmic contacts. The photonic crystal was designed in hexagonal arrays with a period $a=260$ nm and a hole diameter $2r=165$ nm. The PhC mirror has a length of 30 μm and starts at 8 μm away from the edge of the ridge mesa. The holes in the PhC were defined by e-beam lithography and etched by an inductively coupled plasma reactive ion etcher using $SiCl_4/Ar$. The etching went through the laser's active layer and the confining layer and stopped at an $Al_{0.9}Ga_{0.1}As$ sacrificial layer. The slab was then formed by undercutting the sacrificial layer using a selective chemical etch, buffered HF (BOE), through the holes. The thickness of the slab was 600 nm and the air gap was 200 nm. The layer thicknesses used here were chosen for the convenience of fabrication and are probably not optimized for the PhC slab and the nanocavity. But since the cavity is placed quite close to the end of the laser ridge, the effect of the layer thickness on the nanocavity's performance is limited.

The PhC nanocavities were placed at the sixth row of the lattice from the edge of the PhC mirror. The position was chosen to ensure a good coupling from the laser light and a good *Q* factor for the nanocavities. The light intensity and its line shape of the trapped light in a single defect cavity as a function of its position is calculated by the 2D finite-difference time-domain (FDTD) method and shown in Fig. 1(b). Clearly a trade-off between the coupling efficiency and the *Q* factor has to be considered. Based on the calculated result, the location at the sixth row appears to be the best for both good light coupling and a good *Q* factor.

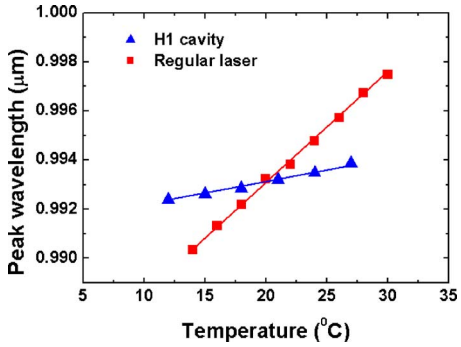

FIG. 3. (Color online) Temperature dependence of the peak wavelength of the laser light measured from an H1 nanocavity and that of the regular laser light measured from the cleaved facet. The slopes of these two lines are 0.097 nm/°C (blue triangle) and 0.45 nm/°C (red square), respectively.

Lasers with two types of nanocavities, H1 and H2, were fabricated, where H1 being the single defect cavity with only one hole removed and H2 being the cavity with seven holes removed, as shown in the inset of Fig. 2(a). Guided by the calculation result shown in Fig. 1(b), we placed the cavities at the sixth row of the PhC mirror for optimum light coupling. Numerical calculation of the band structure and the field distribution profiles indicate that, within the laser's gain bandwidth, the resonant modes for the H1 and H2 cavities are monopole mode and dipole mode, respectively [see Fig. 2(b)]. Surface emissions from these nanocavities were monitored and compared with the laser emission from the other end facet. Curves of the light output against injection current from the nanocavity for lasers integrated with H1 and H2 are shown in Fig. 2(a). Clearly the H2 cavity had a higher external quantum efficiency and a slightly higher threshold current than the H1 cavity. This is understandable because the H2 cavity, due to a larger size, has a higher coupling efficiency than the H1 cavity. The increased output coupling in turn causes a slight reduction in the reflectivity of the PhC mirror, and that contributes to the increase of the threshold current.

The spectrum of the laser light emitted from the PhC nanocavity is very different from that measured from the cleaved facet of the laser diode. The nanocavity only picks up the resonant mode with a specific wavelength from the relatively wide laser spectrum. Figure 2(c) shows the spectrum measured from a laser with an H1 cavity and that from a laser with an H2 cavity. The spectrum measured from the H1 cavity peaks at $\lambda=992.8$ nm and has a linewidth of 0.526 nm. The emission from the H2 cavity peaks at a slightly longer wavelength but has a much narrower width of only 0.26 nm. The spectrum from the cleaved mirror of the laser with an H1 cavity was also measured and is shown in Fig. 2(d). It is much wider but has a clear dip at exactly the same position of the H1 cavity's emission peak. This clearly shows that part of the laser power is taken away by the resonant mode of the nanocavity. This phenomenon can be understood by the reflectivity of the PhC with the nanocavity. Because part of the light is coupled into the resonant mode of the nanocavity, the reflectivity spectrum shows a dip at the

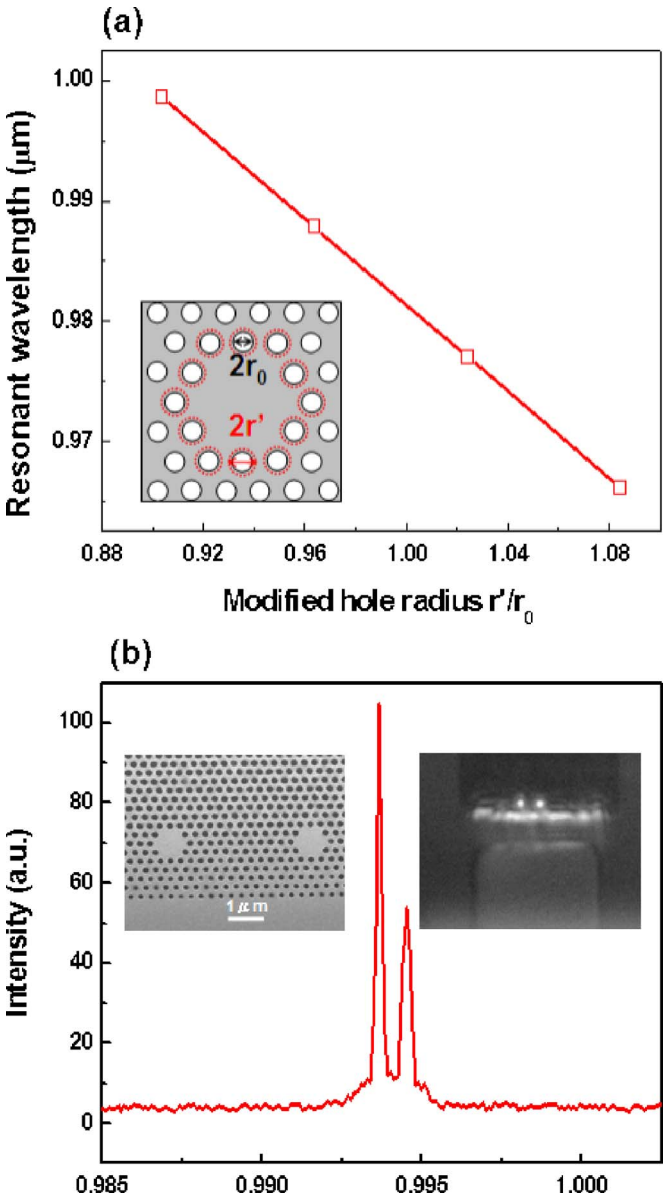

FIG. 4. (Color online) (a) Resonant wavelength as a function of holes radius in modified H2 nanocavities. The inset depicts that 12 inner most holes are modified in diameter. $2r_0$ and $2r'$ denote the diameter of the regular holes and modified innermost holes, respectively. (b) Measured spectrum of the laser light from the two nanocavities. The inset: (left) SEM micrograph of two side by side modified H2 PhC nanocavities; (Right) infrared image of laser emission from the two nanocavities.

resonant wavelength and this results in a reduced emission intensity for the laser light from the cleaved mirror at that wavelength.

From the linewidths obtained, we calculated the Q factors for the H1 and H2 cavities to be 1890 and 3800, respectively. The higher Q for the H2 nanocavity is due to its nondegenerate monopole mode.

The temperature sensitivity of the emission peak from the PhC nanocavities is much better than that from the cleaved facet of Fabry-Pérot lasers without any PhC structures. Figure 3 shows the temperature dependence of the emission peak from a laser with an H1 nanocavity and that of a laser without the PhC mirror. The amount of wavelength shift per °C for the regular laser is 0.45 nm/°C, but that from the H1 nanocavity is only 0.097 nm/°C. There is nearly a five times difference between the two. This also demonstrates the advantage of using the PhC nanocavity as the light source.

The emission wavelength of PhC nanocavities can be easily tuned by cavity design. By slightly changing the size of the innermost holes of a cavity, we can shift the resonant wavelength of the cavity continuously. Figure 4(a) shows the calculated wavelength shift of an H2 nanocavity. The rate of shift $\Delta\lambda/2\Delta r'$ is −1.08 nm/nm. Based on this result, we designed two H2 nanocavities side by side. The cavities had a=260 m, $2r$=166 nm. One of the cavities had all the surrounding holes the same dimension as the rest of the holes in the photonic crystal, while the other one had the surrounding holes (the inner most holes) slightly smaller with the diameter $2r'$=165.2 nm. The left and right insets in Fig. 4(b) show the scanning electron microscopy (SEM) micrograph of the two fabricated nanocavities and the infrared image of the surface emitting laser beam from these nanocavities. Also the spectrum of the laser light from the two cavities is shown in Fig. 4(b). Two narrow emission peaks corresponding to the two cavities at 993.4 and 994.2 nm are clearly seen. The separation of the two peaks is 0.8 nm.

In conclusion, we have fabricated an integrated PhC nanocavity-laser structure. The 2D PhC slab was used as one of the reflective mirrors for the laser cavity, while the nanocavity in the photonic crystal serves as a coupling outlet for the surface emitting laser light. In this manner, an electrically driven laser light is converted to a surface emitting laser light with a narrow spectrum. Both H1 and H2 nanocavities have been fabricated. Single mode emission with high Q factors [Q(H1)=1890 and Q(H2)=3800] was obtained. Excellent temperature stability (0.097 nm/°C) of the laser emission from the nanocavity was observed as well. We have also demonstrated the multiple wavelength emission capability of this integrated structure by utilizing two PhC nanocavities with slightly different designs. Two single modes, narrow linewidth surface emitting laser lights were obtained. This opens up a new possibility of using PhC nanocavities for WDM applications.

[1]S. John, Phys. Rev. Lett. **58**, 2486 (1987).
[2]E. Yablonovitch, Phys. Rev. Lett. **58**, 2059 (1987).
[3]S. Noda, A. Chutinan, and M. Imada, Nature (London) **407**, 608 (2000).
[4]L. Wu, M. Mazilu, T. Karle, and T. F. Krauss, IEEE J. Quantum Electron. **38**, 915 (2002).
[5]T. Baba, A. Motegi, T. Iwai, N. Fukaya, Y. Watanabe, and A. Sakai, IEEE J. Quantum Electron. **38**, 743 (2002).
[6]A. Gomyo, J. Ushida, M. Shirane, M. Tokushima, and H. Yamada, IEICE Trans. Electron. **E87-C**, 328 (2004).
[7]M. F. Yanik, S. Fan, and M. Soljacic, Appl. Phys. Lett. **83**, 2739 (2003).
[8]T. Tanabe, M. Notomi, A. Shinya, S. Mitsugi, and E. Kuramochi, Opt. Lett. **30**, 2575 (2005).
[9]A. Shinya, S. Mitsugi, T. Tanabe, M. Notomi, Y. Yokohama, H. Takara, and S. Kawanish, Opt. Express **14**, 1230 (2006).
[10]K. Seinivasan and O. Painter, Opt. Express **10**, 670 (2002).
[11]Y. Akahane, T. Asano, B. S. Song, and S. Noda, Nature (London) **425**, 944 (2003).
[12]H. Y. Ryu, M. Notomi, G. H. Kim, and Y. H. Lee, Opt. Express **12**, 1708 (2004).
[13]O. Painter, R. K. Lee, A. Yariv, A. Sherer, J. D. O'Brien, P. D. Dapkus, and I. Kim, Science **284**, 1819 (1999).
[14]H. G. Park, S. H. Kim, S. H. Kwon, Y. G. Ju, J. K. Yangatu, J. H. Baek, S. B. Kim, and Y. H. Lee, Science **305**, 1444 (2004).
[15]C. Manolatou, M. J. Khan, S. Fan, P. R. Villeneuve, H. A. Haus, and J. D. Joannopoulos, IEEE J. Quantum Electron. **35**, 1322 (1999).
[16]B. S. Song, T. Asano, Y. Akahane, Y. Tanaka, and S. Noda, J. Lightwave Technol. **23**, 1449 (2005).
[17]A. Shinya, S. Mitsugi, E. Kuramochi, and M. Notomi, Opt. Express **13**, 4202 (2005).